Direct momentum imaging of charge transfer following site-selective ionization

Felix Allum,[1,2,3,*] Yoshiaki Kumagai,[4] Kiyonobu Nagaya,[5] James Harries,[6] Hiroshi Iwayama,[7,8] Mathew Britton,[2] Philip H. Bucksbaum,[2] Michael Burt,[1] Mark Brouard,[1] Briony Downes-Ward,[9] Taran Driver,[3] David Heathcote,[1] Paul Hockett,[10] Andrew J. Howard,[2] Jason W. L. Lee,[11] Yusong Liu,[2] Edwin Kukk,[12] Joseph W. McManus,[1] Dennis Milsesevic,[1] Akinobu Niozu,[13] Johannes Niskanen,[12] Andrew J. Orr-Ewing,[14] Shigeki Owada,[15,16] Patrick A. Robertson,[1] Artem Rudenko,[17] Kiyoshi Ueda,[18] James Unwin,[1] Claire Vallance,[1] Tiffany Walmsley,[1] Russell S. Minns,[9] Daniel Rolles,[17] Michael N. R. Ashfold,[14] and Ruaridh Forbes[3,†]

[1] *Chemistry Research Laboratory, Department of Chemistry, University of Oxford, Oxford OX1 3TA, UK*
[2] *PULSE Institute, SLAC National Accelerator Laboratory, 2575 Sand Hill Road, Menlo Park, CA 94025, USA*
[3] *Linac Coherent Light Source, SLAC National Accelerator Laboratory, 2575 Sand Hill Road, Menlo Park, CA 94025, USA*
[4] *Department of Applied Physics, Tokyo University of Agriculture and Technology, Tokyo, Japan*
[5] *Department of Physics, Kyoto University, Kyoto 606-8502, Japan*
[6] *QST, SPring-8, Kouto 1-1-1, Sayo, Hyogo, Japan*
[7] *Institute for Molecular Science, Okazaki 444-8585, Japan*
[8] *Sokendai (The Graduate University for Advanced Studies), Okazaki 444-8585, Japan*
[9] *School of Chemistry, University of Southampton, Highfield, Southampton SO17 1BJ, UK*
[10] *National Research Council of Canada, 100 Sussex Dr. Ottawa, ON K1A 0R6, Canada*
[11] *Deutsches Elektronen-Synchrotron DESY, Hamburg, Germany*
[12] *Department of Physics and Astronomy, University of Turku, FI-20014 Turku, Finland*
[13] *Graduate School of Advanced Science and Engineering, Hiroshima University, Higashi-Hiroshima 739-8526, Japan*
[14] *School of Chemistry, University of Bristol, Cantock's Close, Bristol BS8 1TS, UK*
[15] *RIKEN SPring-8 Center, Sayo, Hyogo, 679-5148, Japan*
[16] *Japan Synchrotron Radiation Research Institute, Hyogo, Japan*
[17] *J.R. Macdonald Laboratory, Department of Physics, Kansas State University, Manhattan, Kansas 66506, USA*
[18] *Department of Chemistry, Tohoku University, Sendai 980-8578, Japan*

(Dated: August 31, 2023)

We study ultrafast charge rearrangement in dissociating 2-iodopropane (2-C_3H_7I) using site-selective core-ionization at the iodine atom. Clear signatures of electron transfer between the neutral propyl fragment and multiply charged iodine ions are observed in the recorded delay-dependent ion momentum distributions. The detected charge transfer pathway is only favorable within a small (few angstrom), charge-state-dependent spatial window located at C-I distances longer than that of the neutral ground-state molecule. These results offer new insights into the physics underpinning charge transfer in isolated molecules and pave the way for a new class of time-resolved studies.

Charge rearrangement within and between molecules is of fundamental importance throughout physics [1–5], chemistry [6–8] and biology [9, 10]. Detailed studies of isolated gas phase molecules offer a powerful route to probing the mechanistic basis of such phenomena. Recent advances in free-electron lasers (FELs) have yielded sources of intense, coherent pulses of X-ray and extreme ultraviolet (XUV) light [11–13], capable of targeting individual atomic orbitals within molecules [14–18]. Multiple ionization at a specific atomic site creates a highly localized charge from which charge transfer (CT) may proceed. This is closely related to collisional CT between multiply charged ions and neutrals which is of astrophysical significance, for instance as the source of electronically excited ions that can cause X-ray emissions from comets and solar winds [2–5].

In pioneering work, Erk *et al.* dissociatively ionized CH_3I using a strong near-infrared laser field, prior to ionizing the departing iodine atom with a FEL-based X-ray probe pulse [1]. Observed low-momentum I^{n+} ions were assigned to site-selective ionization of the departing iodine fragment. This feature's appearance was delayed from the time of the pump excitation, and this delay increased for higher iodine charge states. The n-dependent, delayed onset of this feature is a consequence of CT: when the iodine is multiply ionized to $I^{(n+1)+}$ at short pump-probe delays, positive charge can transfer to the recoiling CH_3 fragment. Both fragments are now positively charged and Coulombically repel, yielding higher-momentumI^{n+} ions and consequently quenching low-momentum $I^{(n+1)+}$ ion production. For higher iodine charge states, this CT can occur over greater internuclear separations

* fallum@stanford.edu
† ruforbes@stanford.edu

(thus, longer pump-probe delays), as qualitatively predicted by the classical over-the-barrier modelv[1, 19, 20]. In short, the over-the-barrier model considers the Coulombic potential between the two sites for a range of internuclear separations. As internuclear distance increases, the Coulombic barrier between the two sites increases, leading to the concept of a charge-state-dependent 'critical distance', at which this barrier is equal to the binding energy of the transferring valence electron. Beyond this distance, the electron transfer is considered forbidden. A more detailed account of the over-the-barrier model is given in Section V of the Supplemental Material (SM). Follow-up work hasvexamined CT in a series of halogenated molecules using, for the pump step, either multiphoton ionization or single-photon UV-induced dissociation analyzing this delayed low-momentum ion feature [18, 21–24].

In principle, delay-dependent momentum distributions of the repelling ions produced from CT and subsequent Coulomb repulsion are richly informative, encoding information about the geometry at the point of CT and the number of electrons transferred. However, such signal could not be isolated in previous experiments, due to its overlap with signal from probe-only Coulomb explosion of unpumped molecules [21, 23, 24], or from Coulombically repelling species produced by probing a dissociative ionization [1, 18]. Here, we present results from an experimental investigation into CT within dissociating 2-iodopropane molecules, in which the Coulombically repelling fragments produced by single charge transfer are isolated and analyzed in detail. We identify narrow regions of interfragment separation at which this CT channel occurs, map how this varies with iodine charge state and observe evidence for nuclear motion after site-selective ionization yet prior to CT.

Molecules of 2-iodopropane were photoexcited by a ∼100 fs ultraviolet (UV) laser pulse with a 267 nm central wavelength, prior to ionization by a ∼30 fs 95 eV XUV laser pulse produced by the SACLA soft X-ray FEL [25]. UV photoabsorption initiates prompt photodissociation of 2-iodopropane by populating repulsive potential energy surfaces (PESs) following a $n_I \rightarrow \sigma_{C-I}^*$ transition [26, 27].

Atomic Xe and molecular C_3H_8 (logical analogues of atomic I and C_3H_7) have photoabsorption cross-sections of ∼25 Mb [28] and ∼1.3 Mb [29], respectively, at 95 eV. Ionization is thus expected to occur selectively at the iodine atom, with the initial I 4d ionization depositing either two or three total positive charges on the molecule (in an approximately 2:1 ratio [28]) following Auger-Meitner (AM) decay(s) [50]. The observation of I^{n+} ions with n as high as 6 in the present study therefore indicates that multiple photoabsorptions can occur. Following site-selective ionization, positive charge may either remain localized at the iodine, or transfer to the neutral alkyl fragment and induce Coulombic repulsion and an increase in the iodine ion momentum. These processes are shown schematically in Fig. 1(a).

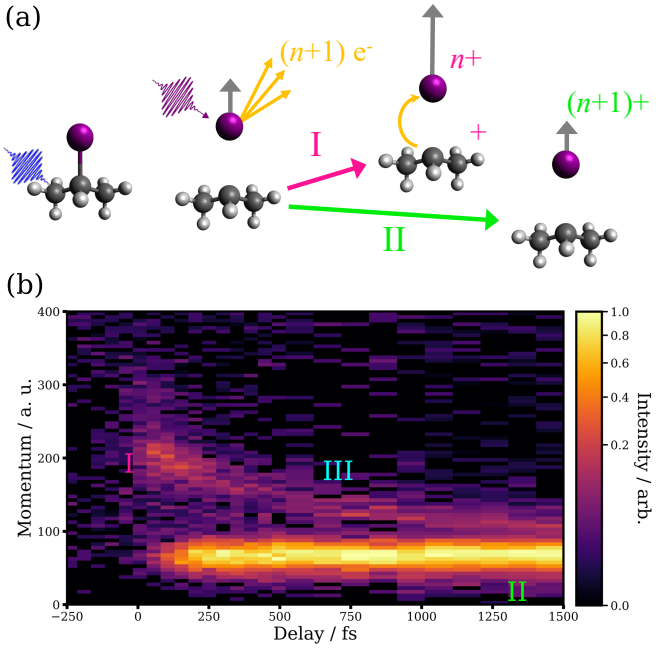

FIG. 1. (a) Experimental schematic, showing UV-induced neutral C-I bond fission in 2-iodopropane followed by site-selective multiple ionization at the iodine atom to its $(n+1)+$ charge state and two possible outcomes, in which either an electron is transferred between fragments (pathway I) or charge remains localized at the iodine (pathway II). The momentum of the iodine ion is indicated by the gray arrow. (b) Momentum distribution in atomic units (a.u.) of the I^{4+} ion as a function of delay between the UV pump and XUV probe lasers. Positive (negative) delays correspond to the UV pulse arriving first (second). In this plot and throughout the manuscript, XUV-only contributions have been removed by subtracting scaled averaged data before time-zero. Data prior to subtraction are shown in the SM. Three distinct pump-probe features are observed, labelled I-III (see text).

The three-dimensional momenta of ionic fragments were recorded in a velocity-map imaging [30] spectrometer [31] as a function of the jitter-corrected pump-probe delay [32].

Figure 1(b) shows the recorded delay-dependent I^{4+} momentum distribution. Three pump-probe features are recognized. Promptly after time-zero, a transient enhancement is observed in the higher-momentum region labelled 'I'. The strongest feature, 'II', exhibits a constant low momentum, appears shortly after time-zero and persists to long pump-probe delays. A weaker feature, 'III', appears after time-zero and exhibits a momentum which decreases with increasing delay. Analogous features are observed for all multiply charged $I^{(2-6)+}$ ions observed (although I^{3+} is excluded from most of the analysis due to its overlapping mass-to-charge ratio with $C_3H_7^+$), as shown in the SM.

Channels I to III may be assigned to the following processes following UV photoexcitation:

I: Site-selective XUV ionization at the iodine atom

to produce $I^{(n+1)+}$ ions, followed by CT to the neutral propyl cofragment to yield I^{n+} and $C_3H_7^+$ (and potentially any smaller fragments derived therefrom) at the earliest stages of C-I bond extension, which Coulombically repel.

II: Site-selective XUV ionization at the departing iodine atom without subsequent CT.

III: XUV ionization of both the separating iodine and propyl fragments, producing a multiply charged iodine ion and a singly charged alkyl cofragment.

Note, the images obtained in this study are for iodine ions in a specific final charge state. An I^{n+} image necessarily reports on parent molecules initially promoted to the $(n+1)+$ charge state in the case of Channel I, but on I atoms promoted to just the $n+$ charge state in the case of Channels II and III.

The momentum and angular distributions of the Channel II products agree well with literature measurements of the neutral UV photodissociation of 2-iodopropane [26], as the XUV ionization process does not substantially alter the momentum of the recoiling iodine fragment. The significantly greater momenta of Channels I and III arise from Coulomb repulsion against a singly charged alkyl fragment, which decreases for longer pump-probe delays (greater internuclear separations) [33, 34]. As shown in Fig S3 of the SM, Channels I and II exhibit very similar photoion angular distributions, supporting their assignment to the same single-photon UV-induced photodissociation. Channel II exhibits a delayed appearance relative to Channel I, implying that, at earlier pump-probe delays where the iodine atom is close to the propyl fragment, CT is favored, but becomes improbable at longer pump-probe delays. This cessation of CT, heralding the formation of the low-momentum iodine ions of Channel II, was the primary focus of previous ultrafast CT studies [1], in which the direct signature of CT (Channel I) could not be resolved. As explored shortly, Channel I shares the dependence on ion charge state which has been viewed as characteristic of CT [1, 21].

The ability to observe Channel I in the current work is attributed to two factors. Firstly, the use of a weak-field UV pump pulse drives the excitation of a well-defined neutral dissociation. This is in stark contrast to initial experiments where strong-field pump pulses drove dissociative ionization, generating a large Coulomb explosion background [1, 18]. Secondly, by studying a larger molecule (C_3H_7I as opposed to CH_3I), there are more atoms to carry charge in XUV-only Coulomb explosions, reducing the one-color production of multiply charged I^{n+} ions [23, 35]. For example, a slight enhancement in the yield of high-KER I^{n+} ions shortly after time-zero was assigned to the presence of Channel I in a previous UV-XUV study on CH_3I (see Fig. 8 of Ref 23), but isolation (and thus further analysis) of the feature was not possible due to one-color background.

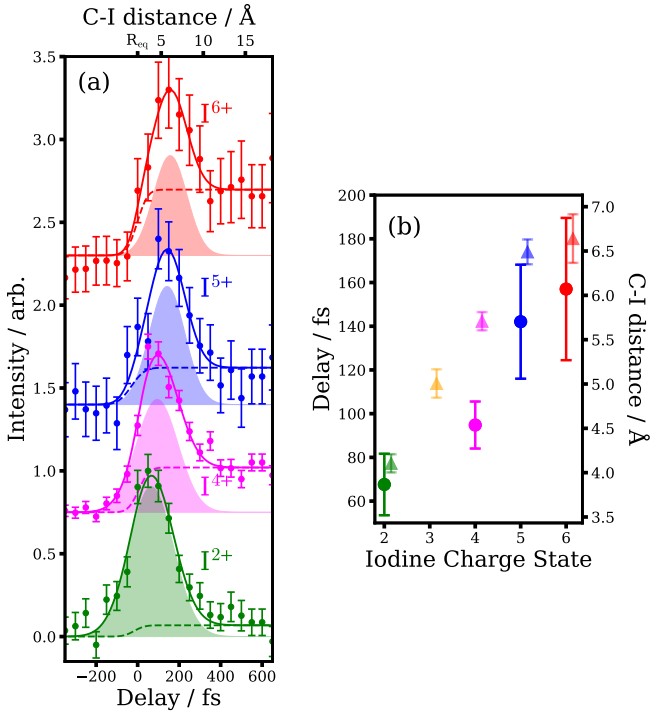

FIG. 2. (a) Integrated intensity of the background-subtracted delay-dependent I^{n+} ion momentum distributions for 120-300 a.u.(colored circles). For the I^{2+} ion, a narrower momentum range of 110 to 200 a.u. was used, to avoid overlap with probe-only signal. Intensities are normalized by their maximum value, and vertically offset. The total fit is plotted as a solid line. The two contributions to this fit, representing signal arising from Channels I and III are displayed as a shaded area and dashed line, respectively. (b) The centers of the Gaussian contributions (round marker) for each iodine charge state, with error bars corresponding to 1 standard deviation (1σ) of the fit parameter. The onsets of Channel II (triangular marker), determined by fitting solely to a normal cumulative distribution function, are shown for comparison.

Analyzing the Channel I signal in both the delay and momentum domains for each iodine charge state informs on how the time of XUV ionization affects the probability for CT, and the geometry at which the CT occurs. Figure 2(a) shows the delay-dependent intensities of high-momentum I^{n+} ions. These comprise a strong contribution from CT (Channel I), as well as a weaker contribution due to simultaneous photoionization at both I and C_3H_7 fragments by the XUV pulse (Channel III). The former process leads to an enhancement in the ~0-300 fs range, whilst the latter is responsible for the increased signal which begins around time-zero and persists out to longer pump-probe delays.

If we assume a single value for the dissociation (i.e., C-I bond extension) velocity following UV photoexcitation at time-zero, the delay axis can directly map to C-I bond length at the instant of inner-shell ionization [1].

This assumption of instantaneous acceleration introduces little error, owing to the very repulsive PESs involved in the photodissociation which cause rapid (∼few tens of fs) acceleration to the asymptotic dissociation velocity [26, 36]. Several interesting features can be observed in Fig. 2. Firstly, the CT peaks shortly after time-zero, at which point significant UV-induced bond extension has already occurred (cf. the ground state equilibrium bond length of ∼2.2 Å). Secondly, the peak in intensity of Channel I is narrow in time (200-300 fs FWHM), and shifts to longer pump-probe delays with increasing charge state n. To examine this trend further, we fit the traces in Fig. 2(a) to a two-component function: i) a Gaussian representing the transient enhancement due to Channel I and ii) a normal cumulative distribution function (CDF), representing the step-like enhancement due to Channel III.

Fig. 2(b) shows that the center of the Gaussian contribution shifts to longer pump-probe delay/C-I bond distances as iodine charge state increases. A corresponding shift in the onset of Channel II (triangular markers in Fig. 2(b)) is also observed, in accord with previous studies [1, 21]. The temporal width of the Gaussian contribution at high ion momentum (i.e., the shaded contribution in Fig. 2(a)) is independent of charge state (within fitting error), indicating that within the constraints of the experimental time resolution (∼120 fs FWHM), the geometric 'window' (i.e. the range of C-I distances at the point of ionization) for CT is approximately equal for each I^{n+}, and it is this entire 'window' which shifts to more extended geometries as n increases.

The precise momentum of the I^{n+} fragments from Channel I encodes information about the molecular geometry at which electron transfer occurred. Under the assumptions of a classical Coulombic repulsion of two point charges between the I^{n+} ion and a singly-charged propyl cofragment, and a single dissociation velocity, an ion's momentum can be transformed directly to a separation between two repelling charges.

We note that such analysis neglects motion in dimensions other than the C-I coordinate and assumes that the Coulombic repulsion can be adequately described by considering two point charges, with the charge of the $C_3H_7^+$ species located on the central carbon atom. The assumption of purely Coulombic repulsion does not generally perform well at short internuclear distances, where the polycation PESs include contributions from valence bonding interactions [37–41]. However, as the CT and subsequent Coulomb explosion happens at extended geometries, the interactions can be well-approximated as those of point charges. Similarly, photoinduced vibrational motion in other coordinates (such as umbrella mode of the propyl radical [26]) is not expected to significantly alter the Coulomb repulsion at the level of sensitivity of the present experiment.

Figure 3 displays early-time (0-300 fs) ion momentum distributions, following transformation to a charge separation assuming Coulombic behavior. Contributions from Channel III have been subtracted, as described in the SM Section VIII, leaving signal arising solely from Channel I. Here, comparison is drawn to the 'critical distance' predicted by the over-the-barrier model. This distance, at which the Coulombic barrier to electron transfer exceeds the valence electron binding energy and so CT is 'classically forbidden', increases with higher iodine charge state due to a deeper Coulombic well [1, 19, 20, 42] (as shown in SM Fig. S9). This comparison highlights observed details of the CT behaviour which cannot be adequately described by this simple model. For instance, in many cases (particularly the higher charged iodine ions), CT has essentially halted before the predicted critical distance, and has a well-defined peak over a narrow region of charge separation, below which single CT is not observed.

Further comparison is drawn to the analysis in the pump-probe delay domain (the shaded contributions to the fits shown in Fig. 2(a), which are reproduced in Fig. 3 as dashed lines), which relates the intensity of Channel I to the C-I distance at the point of ionization (rather than at the point of CT). The momentum-domain analysis yields much narrower distributions, as the geometric information is no longer restricted by the experimental time resolution. The direct comparison shows that,

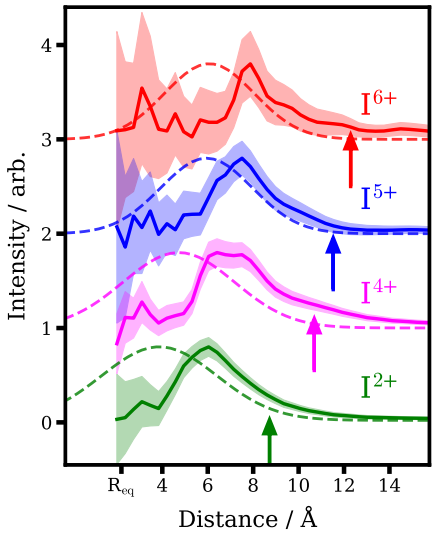

FIG. 3. Yield of Channel I as a function of charge separation as extracted from the I^{n+} ion momentum distributions. These distributions are vertically offset and each normalized by their maximum value. The shaded regions represent estimated 1σ error bars. The relevant critical distance predicted by the over-the-barrier model for the $I^{(n+1)+}$+C_3H_7 to I^{n+}+$C_3H_7^+$ CT process for each charge state n is indicated by a colored arrow. For comparison, the Gaussian distributions of C-I internuclear distances extracted from the delay-domain analysis shown in Fig. 2 are reproduced as dashed lines.

on average, the C-I bond is more extended at the point of CT than at the point of ionization. This observation, which was inaccessible by previous studies, implies that there may be a small time delay between ionization at the I atom and CT, during which the two fragments continue to recoil along the dissociation coordinate. These observations are consistent with CT being mediated by crossings between PESs which occur at specific geometries with more extended C-I bond distances, as discussed shortly.

Whilst the cessation of CT (i.e. onset of Channel II signal) has been probed by previous work involving time-resolved site-selective ionization [1], the present studies provide the first direct measurement of the entire window over which single CT occurs. The signature of CT is absent at the smallest pump-probe delays (smallest C-I bond extensions). This behavior can be interpreted in terms of differing stages in the transition from an intact molecule to isolated photofragments following UV excitation. At sufficiently large C-I bond extension, charge is localized at the isolated iodine atom following ionization. When the C-I bond distance is close to its neutral ground state equilibrium value, XUV ionization again proceeds from the I 4d orbital, but the AM relaxation is molecular in nature, and leads to Coulomb explosion behavior similar to that of the unpumped molecule, in which multiple carbon- and/or hydrogen-containing ionic fragments are produced [35]. Between these two regimes ionization and AM decay is localized at the iodine atom, but the distance from the iodine to the recoiling neutral propyl fragment is small enough that single electron transfer from the propyl is possible. At the shortest pump-probe delays, we appreciate that multiple CTs could conceivably also play a role and persist out to longer pump-probe delays for higher iodine charge states, though the present experiments do not show any clear signatures of such processes. The persistence of multiple CT out to longer pump-probe delay/internuclear distance for higher iodine charge state may explain the observed charge-state-dependent shift in the onset of single CT. In future studies, the incorporation of coincidence or covariance [35] ion detection would be valuable, to distinguish I^{n+} ions formed in the same process as singly charged propyl ions (or their daughter fragments) from those formed with smaller fragment ions that derive from the decay of propyl polycations (the signature of multiple electron transfers).

CT cross-sections, particularly at low collision energies, are dominated by non-adiabatic effects at the crossings of PESs [19, 43]. Many such surface-crossings can contribute to a given CT process, populating a series of electronically excited (Rydberg) states in the polycation accepting the transferred electron (as discussed in more detail in the SM Section X). Future work may be able to 'map out' these regions of non-adiabaticity through complementary delay-dependent measurements on the electronic state of the product I^{n+} ions. Identification of specific electronic pathways through which CTs operate might be achieved through measuring fluorescence spectra of the I^{n+} ions, as reported extensively for collision-induced CT [44–48]. A number of methods exist for predicting the n and l propensities for Rydberg states formed in charge-exchange collisions [20, 44]. In a photodissociating system, however, the motions of the participating systems are much more constrained; the two moities travel away from one another, initially from a very small separation and with a well-defined relative orientation. Such simplicity is in marked contrast to the colliding systems, where the partners first approach from long distance, with a range of impact parameters, and reach some minimum distance of approach before travelling apart again. It is this difference in motions, and the ability for dissociation to be induced at a specific delay before site-selective ionization which could enable new regimes of CT physics to be accessed in these emerging ultrafast pump-probe measurements.

In conclusion, we present an experimental study of CT processes initiated by site-selective inner-shell ionization during a neutral photodissociation. A clear signature of the Coulombically repelling fragments formed by CT between the selectively ionized iodine atom and the recoiling alkyl radical is identified. This CT occurs over a small window of C-I separations which is significantly extended from the equilibrium geometry and shifts to greater internuclear distances for higher I^{n+} charge states. This geometric window corresponds to intermediate behavior in the electronic relaxation dynamics following I 4d ionization between the limits of an isolated iodine atom (at large C-I distance) and that of a bound molecule (at the equilibrium C-I distance), at which point interfragment electron transfer can occur. The propensity for CT to occur over a narrow region of C-I internuclear separation can be understood in terms of couplings between PESs at these specific geometries which mediate CT. We see compelling evidence that, if multiple ionization occurs in the dissociating system at shorter internuclear distances, CT may be delayed until these regions of strong coupling are reached. Future experiments in which photoions and AM electrons are recorded simultaneously and analyzed in coincidence or covariance [36, 49] would be of particular interest to study transient electronic structure changes, as too would the detection of fluorescence produced by radiative relaxation of the electronically excited I^{n+} species produced [44–48].

ACKNOWLEDGMENTS

The experiment was performed at SACLA with the approval of JASRI and the program review committee (proposal No. 2021A8038 Forbes). We thank the technical and scientific staff of SACLA for their hospitality and support before and during the beamtime.

R.F. and F.A. gratefully acknowledge support from the Linac Coherent Light Source, SLAC National Accelerator Laboratory, which is supported by the US Department of Energy, Office of Science, Office of Basic Energy Sciences, under contract no. DE-AC02-76SF00515. D.R. and A.R. were supported by contract no. DE-FG02-86ER13491 from the same funding agency. J.W.L.L. acknowledges financial support via the Helmholtz-ERC Recognition Award (ERC-RA-0043) of the Helmholtz Association (HGF). B.D.W. thanks the CLF and the University of Southampton for a studentship. R.S.M. thanks the EPSRC for financial support (EP/R010609/1). J.M., M.Bro., D.M., D.H., P.A.R., C.V. and A.J.O.E. gratefully acknowledge the support of EPSRC Programme grant EP/V026690/1. M.Bu. and T.W. are also grateful to EPSRC for support from EP/S028617/1. T.W. is additionally thankful to EPSRC for studentship funding and Jesus College, Oxford for a partial fee scholarship. P.H.B., A.J.H. and M.Bri. were supported by the National Science Foundation. J.N. acknowledges Academy of Finland funding via project 331234. Y.K. acknowledges support by JSPS KAKENHI Grant No. 20K14427.

[1] B. Erk, R. Boll, S. Trippel, D. Anielski, L. Foucar, B. Rudek, S. W. Epp, R. Coffee, S. Carron, S. Schorb, *et al.*, Science **345**, 288 (2014).
[2] T. Cravens, Geophys. Res. Lett. **24**, 105 (1997).
[3] T. Cravens, Science **296**, 1042 (2002).
[4] S. Snowden, M. Collier, and K. Kuntz, Astrophys. J. **610**, 1182 (2004).
[5] K. Dennerl, Space Sci. Rev. **157**, 57 (2010).
[6] S. D. Price, M. Manning, and S. R. Leone, J. Am. Chem. Soc. **116**, 8673 (1994).
[7] S. D. Price, Int. J. Mass. Spectrom. **260**, 1 (2007).
[8] S. D. Price, J. D. Fletcher, F. E. Gossan, and M. A. Parkes, Int. Rev. Phys. Chem. **36**, 145 (2017).
[9] R. A. Marcus and N. Sutin, Biochim. Biophys. Acta - Bioenerg. **811**, 265 (1985).
[10] A. M. Kuznetsov, *Charge transfer in physics, chemistry and biology: physical mechanisms of elementary processes and an introduction to the theory* (CRC Press, 2020).
[11] J. Feldhaus, J. Phys. B: At. Mol. Opt. Phys. **43**, 194002 (2010).
[12] P. Emma, R. Akre, J. Arthur, R. Bionta, C. Bostedt, J. Bozek, A. Brachmann, P. Bucksbaum, R. Coffee, F.-J. Decker, *et al.*, Nat. Photonics **4**, 641 (2010).
[13] T. Ishikawa, H. Aoyagi, T. Asaka, Y. Asano, N. Azumi, T. Bizen, H. Ego, K. Fukami, T. Fukui, Y. Furukawa, *et al.*, Nat. Photonics **6**, 540 (2012).
[14] H. Fukuzawa, S.-K. Son, K. Motomura, S. Mondal, K. Nagaya, S. Wada, X.-J. Liu, R. Feifel, T. Tachibana, Y. Ito, *et al.*, Phys. Rev. Lett. **110**, 173005 (2013).
[15] B. Erk, D. Rolles, L. Foucar, B. Rudek, S. W. Epp, M. Cryle, C. Bostedt, S. Schorb, J. Bozek, A. Rouzee, *et al.*, Phys. Rev. Lett. **110**, 053003 (2013).
[16] F. Braußе, G. Goldsztejn, K. Amini, R. Boll, S. Bari, C. Bomme, M. Brouard, M. Burt, B. C. De Miranda, S. Düsterer, *et al.*, Phys. Rev. A **97**, 043429 (2018).
[17] M. Ilchen, P. Schmidt, N. M. Novikovskiy, G. Hartmann, P. Rupprecht, R. N. Coffee, A. Ehresmann, A. Galler, N. Hartmann, W. Helml, *et al.*, Commun. Chem. **4**, 1 (2021).
[18] F. Allum, N. Anders, M. Brouard, P. Bucksbaum, M. Burt, B. Downes-Ward, S. Grundmann, J. Harries, Y. Ishimura, H. Iwayama, *et al.*, Faraday Discuss. **228**, 571 (2021).
[19] H. Ryufuku, K. Sasaki, and T. Watanabe, Phys. Rev. A **21**, 745 (1980).
[20] A. Niehaus, J. Phys. B: At. Mol. Opt. Phys. **19**, 2925 (1986).
[21] R. Boll, B. Erk, R. Coffee, S. Trippel, T. Kierspel, C. Bomme, J. D. Bozek, M. Burkett, S. Carron, K. R. Ferguson, *et al.*, Struct. Dyn. **3**, 043207 (2016).
[22] K. Amini, E. Savelyev, F. Braußе, N. Berrah, C. Bomme, M. Brouard, M. Burt, L. Christensen, S. Düsterer, B. Erk, *et al.*, Struct. Dyn. **5**, 014301 (2018).
[23] R. Forbes, F. Allum, S. Bari, R. Boll, K. Borne, M. Brouard, P. H. Bucksbaum, N. Ekanayake, B. Erk, A. J. Howard, *et al.*, J. Phys. B: At. Mol. Opt. Phys. **53**, 224001 (2020).
[24] H. Köckert, J. Lee, F. Allum, K. Amini, S. Bari, C. Bomme, F. Braußе, M. Brouard, M. Burt, B. C. de Miranda, *et al.*, J. Phys. B: At. Mol. Opt. Phys. (2022).
[25] S. Owada, K. Togawa, T. Inagaki, T. Hara, T. Tanaka, Y. Joti, T. Koyama, K. Nakajima, H. Ohashi, Y. Senba, T. Togashi, K. Tono, M. Yamaga, H. Yumoto, M. Yabashi, H. Tanaka, and T. Ishikawa, J. Synchrotron Radiat. **25**, 282 (2018).
[26] M. E. Corrales, V. Loriot, G. Balerdi, J. González-Vázquez, R. de Nalda, L. Banares, and A. H. Zewail, Phys. Chem. Chem. Phys. **16**, 8812 (2014).
[27] M. A. Todt, S. Datta, A. Rose, K. Leung, and H. F. Davis, Phys. Chem. Chem. Phys. **22**, 27338 (2020).
[28] N. Saito and I. H. Suzuki, Int. J. Mass Spectrom. Ion Process. **115**, 157 (1992).
[29] J. W. Au, G. Cooper, G. R. Burton, T. N. Olney, and C. Brion, Chem. Phys. **173**, 209 (1993).
[30] A. T. J. B. Eppink and D. H. Parker, Rev. Sci. Instrum. **68**, 3477 (1997),.
[31] H. Fukuzawa, K. Nagaya, and K. Ueda, Nucl. Instrum. Methods Phys. Res. A: Accel. Spectrom. Detect. Assoc. Equip. **907**, 116 (2018),.
[32] S. Owada, K. Nakajima, T. Togashi, T. Katayama, H. Yumoto, H. Ohashi, and M. Yabashi, J. Synchrotron Radiat. **26**, 887 (2019).
[33] H. Stapelfeldt, E. Constant, and P. Corkum, Phys. Rev. Lett. **74**, 3780 (1995).
[34] F. Allum, M. Burt, K. Amini, R. Boll, H. Köckert, P. K. Olshin, S. Bari, C. Bomme, F. Braußе, B. Cunha de Miranda, *et al.*, J. Chem. Phys. **149**, 204313 (2018).
[35] J. W. McManus, T. Walmsley, K. Nagaya, J. R. Harries, Y. Kumagai, H. Iwayama, M. N. Ashfold, M. Britton, P. H. Bucksbaum, B. Downes-Ward, *et al.*, Phys. Chem. Chem. Phys. **24**, 22699 (2022).

[36] F. Allum, V. Music, L. Inhester, R. Boll, B. Erk, P. Schmidt, T. M. Baumann, G. Brenner, M. Burt, P. V. Demekhin, *et al.*, Commun. Chem. **5**, 1 (2022).
[37] C. Ellert, H. Stapelfeldt, E. Constant, H. Sakai, J. Wright, D. Rayner, and P. Corkum, Philos. Trans. Royal Soc. A **356**, 329 (1998).
[38] J. S. Wright, G. DiLabio, D. Matusek, P. Corkum, M. Y. Ivanov, C. Ellert, R. Buenker, A. Alekseyev, and G. Hirsch, Phys. Rev. A **59**, 4512 (1999).
[39] F. Penent, P. Lablanquie, J. Palaudoux, L. Andric, G. Gamblin, Y. Hikosaka, K. Ito, and S. Carniato, Phys. Rev. Lett. **106**, 103002 (2011).
[40] M. E. Corrales, G. Gitzinger, J. González-Vázquez, V. Loriot, R. de Nalda, and L. Banares, J. Phys. Chem. A **116**, 2669 (2012).
[41] S. W. Crane, L. Ge, G. A. Cooper, B. P. Carwithen, M. Bain, J. A. Smith, C. S. Hansen, and M. N. Ashfold, J. Phys. Chem. A **125**, 9594 (2021).
[42] R. Mann, F. Folkmann, and H. Beyer, J. Phys. B: At. Mol. Opt. Phys. **14**, 1161 (1981).
[43] H. Ryufuku and T. Watanabe, Phys. Rev. A **18**, 2005 (1978).
[44] P. Beiersdorfer, R. Olson, G. Brown, H. Chen, C. Harris, P. Neill, L. Schweikhard, S. Utter, and K. Widmann, Phys. Rev. Lett. **85**, 5090 (2000).
[45] J. Greenwood, I. Williams, S. Smith, and A. Chutjian, Phys. Rev. A **63**, 062707 (2001).
[46] S. Bliman, R. Bruch, M. Cornille, A. Langereis, and J. Nordgren, Phys. Rev. A **66**, 052707 (2002).
[47] P. Beiersdorfer, K. Boyce, G. Brown, H. Chen, S. Kahn, R. Kelley, M. May, R. Olson, F. Porter, C. Stahle, *et al.*, Science **300**, 1558 (2003).
[48] S. Otranto, R. E. Olson, and P. Beiersdorfer, Phys. Rev. A **73**, 022723 (2006).
[49] F. Allum, C. Cheng, A. J. Howard, P. H. Bucksbaum, M. Brouard, T. Weinacht, and R. Forbes, J. Phys. Chem. Lett. **12**, 8302 (2021).
[50] D. Matsakis, A. Coster, B. Laster, and R. Sime, Phys. Today **72**, 10 (2019), and references therein.